

Correlative multiscale tomography of biological materials

Robert S. Bradley and Philip J. Withers

The intricate hierarchical microstructures typical of biological materials give rise to fascinating combinations of anisotropic mechanical properties that can surpass those of man-made materials. The linking together of three-dimensional (3D) imaging techniques has the potential to reveal these structures in unprecedented detail. However, a complete understanding can only be reached if the relationship between structure and mechanical properties can be elucidated. X-ray-computed tomography (CT) is uniquely placed to image such structures across a wide range of length scales. We review recent technical advances that are leading to improved contrast and spatial resolution. We highlight how time-lapse CT 3D studies can track the response of hierarchical microstructures to mechanical loading.

Introduction

Biological materials are generally characterized as having complex three-dimensional (3D) hierarchical microstructures,[1] giving rise to interesting combinations of anisotropic mechanical properties that, in many cases, surpass those of man-made materials.[2] Consequently, much can be learned from a detailed study of their structure–property relationships.[3] As discussed by Vincent,[4] these materials are often composites of organic and inorganic components that exploit strong fibers, such as cellulose (e.g., wood, spider silk, and cuticle), or ceramics based around calcium carbonate (e.g., nacre), silica (e.g., the skeleton of *Euplectella*, a genus of deep water sponges), or hydroxyapatite (e.g., bone).[5] The resultant combinations of properties are all the more surprising since the constituent components typically exhibit relatively ordinary properties in isolation.[6] The overall properties of biological materials rely on the use of hard and soft materials in combination with carefully controlled interfacial properties, as well as morphological optimization across many length scales, as illustrated in **Figure 1**.

A better understanding of these hierarchical structures requires a multiscale correlative imaging approach, which brings together 3D information at each length scale.[7] Multiscale imaging is highly challenging because no single technique can provide all the information. Optical techniques are suitable for translucent tissues,[8] while 3D scanning electron microscopy (SEM) serial sectioning techniques achieve resolutions of tens of nanometers, but only over 100-µm volumes, and are not amenable to temporal 3D studies of the same specimen. In this respect, x-ray computed tomography (CT) is uniquely placed as a noninvasive technique able to provide 3D images across a wide range of resolutions from hundreds of micrometers to tens of nanometers. However, the technique has traditionally been limited by poor contrast for soft tissues.

A further challenge for biological imaging is the x-ray dose. For *in vivo* imaging of mammals, the dose needs to be limited to <10 Gy, although it can be much higher (>1.5 kGy) for insects, which are much more radiation tolerant.[9] In general, the required dose to achieve a given contrast-to-noise ratio increases as the fourth power of resolution.[10] Higher doses can be used for *ex vivo* samples, with cryo-preservation techniques able to mitigate against dose effects for imaging down to ~30-nm resolution.[11] Higher resolutions can be achieved by coherent diffraction imaging techniques ("lensless" imaging). Howells et al.[10] postulated that an ultimate dose limit exists due to damage to proteins of ~10^8 Gy per nanometer of resolution.

This article reviews recent advances in x-ray imaging techniques for studying the role of hierarchical structures in controlling the mechanical behavior of biomaterials. In particular, new opportunities to study the relationship between microstructurally controlled propagation of damage and performance through time-lapse 3D imaging are highlighted.

Robert S. Bradley, The University of Manchester, UK; rob.bradley@geotek.co.uk
Philip J. Withers, School of Materials, The University of Manchester, UK; p.j.withers@manchester.ac.uk
doi:10.1557/mrs.2016.137

© 2016 Materials Research Society

https://doi.org/10.1557/mrs.2016.137 Published online by Cambridge University Press

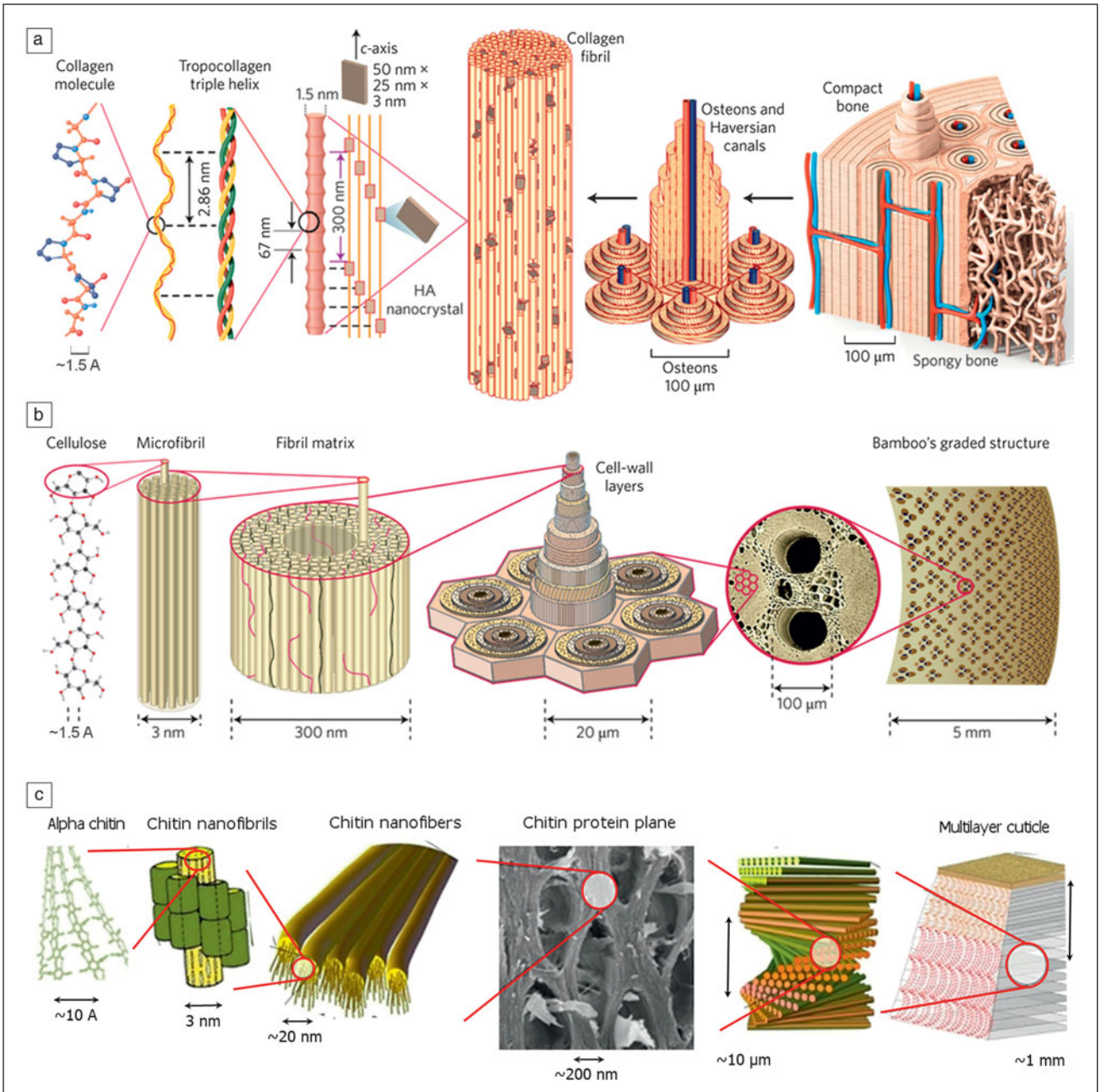


Figure 1. Levels of hierarchy in (a) bone, (b) bamboo, and (c) lobster cuticle. Adapted with permission from References 66 and 67. © 2015 Macmillan Publishers Ltd. and © 2015 Frontiers Media, respectively. Note: HA, hydroxyapatite.

Increased contrast for soft tissue

Phase-contrast x-ray tomography

Phase-imaging techniques make use of the real part of a material's refractive index. At hard x-ray energies, this can be a factor of 1000 greater than that of the complex part, which gives rise to absorption.[12] Phase-contrast methods include free-space propagation,[13] grating interferometry,[14] Zernike phase contrast,[15] and analyzer-based[16] methods. The free-space propagation method is the simplest and requires a coherent, or partially coherent, x-ray source (from a synchrotron, or laboratory x-ray tube having a small spot size) and a relatively large distance between sample and detector. Refraction of x-rays at interfaces within the sample is then manifested as fringes in the radiographs, leading to "edge-enhancement." Walton et al.[17] used this technique to elucidate changes in artery wall architecture between the pressurized and unpressurized states, albeit in an *ex situ* study looking at fixed samples. This type of phase contrast has also been employed for studying novel tissue engineering materials, such as bioglasses.[18]

More advanced techniques measure the phase shift through the object by encoding wavefront distortions in changes in the intensity profile using a mask. Pfeiffer et al.[19] showed that this

https://doi.org/10.1557/mrs.2016.137 Published online by Cambridge University Press

type of imaging can be carried out using conventional low-brilliance x-ray tubes. The resolution is currently limited by difficulties in fabricating fine gratings down to ~10 μm. Schultz et al. reported ~16-μm spatial resolution imaging of a human cerebellum.[20] A number of competing techniques, including speckle and edge-illumination techniques, are being developed that have simpler setups and can achieve higher resolutions. These techniques have recently been shown to work well with conventional laboratory x-ray sources.[16,21,22]

At much higher resolutions, phase-contrast nanotomography using the holography approach has enabled the hierarchical structure of bone to be imaged, with information gained about mineralization and collagen orientations down to ~60-nm resolution.[23] X-ray microscopes make use of Zernike phase contrast. Walton et al.[17] used this technique to visualize small-scale fiber bundles within rat artery walls in 3D at 150-nm resolution (see **Figure 2**).

Coherent diffraction imaging (CDI) can theoretically achieve 10-nm resolution or better by using a "lensless" approach.[24] This has enabled the ultrastructure of collagen to be determined in intact tendons, including the measurement of the periodic spacing of collagen molecules within fibrils.[25] CDI can be used in a scanning mode, termed ptychography, to image relatively large nonisolated objects, and can also be combined with tomography to yield 3D information to study, for example, 3D mineral distributions in dentin,[26] the lacuno-canalicular network in bone (the network of spaces in which cells reside),[27] and the structure of cells[28] and chromosomes.[29]

Contrast agents

The alternative to phase-imaging techniques is to improve absorption contrast by a variety of high atomic number (Z)-contrast agents. Metscher et al.[30] compared a range of stains for developmental biology, finding that inorganic iodine imparts good contrast for most samples, while phosphotungsic acid (PTA) is more selective as it preferentially binds to collagen and other proteins. PTA has been used to image mouse articular cartilage to inform computer models of joint mechanics.[31] Iodine has been used for a variety of tissues, including the heart,[32,33] tendon,[34] liver, and kidneys.[35] However, staining can take many hours, or even days, in order to achieve satisfactory contrast for large specimens,[32] which means that soft tissues need to be chemically fixed to avoid degradation. While fixation can help with the uptake of contrast agents,[30] it involves the cross-linking of proteins, which changes the mechanical properties of the tissue and, ultimately, limits the use of contrast agents in 4D studies.

There is a clear need for more targeted agents that can highlight particular features or structures of interest. High-Z nanoparticles show promise as contrast agents and are actively being investigated for medical imaging.[36–38] Their properties can be enhanced by surface modification by attaching targeting moieties, adding coatings to reduce toxicity, and attaching fluorescent markers for multimodal sensing. While this research is still in its infancy, actively targeted gold nanoparticles have been developed for imaging cancer cells as well as microcalcifications (calcium deposits) in breast tissue and atherosclerotic plaques in arteries.[36] For subcellular imaging, such nanoparticles can also facilitate alignment of nanotomography scans and enable correlation with fluorescence microscopy.[39]

Soft x-ray microscopy

The intrinsic absorption contrast of tissues can be improved by using lower x-ray energies. Soft x-ray microscopes (SXMs) operate in the "water window" (284–543 eV), between the absorption edges of oxygen and carbon, and can achieve excellent absorption contrast of subcellular components. Further, soft x-ray beams are more easily manipulated using lenses, enabling high resolutions to be achieved (down to 10 nm).[40] However, even for soft tissue at these energies, x-rays can only penetrate samples up to ~15-μm thickness, so 3D imaging is typically achieved via limited-angle tomography (projections collected over a range of angles <180°). Recently, the technique has been transferred from the synchrotron to laboratory systems.[41,42] The greatest advantage of SXMs is when they are combined with cryopreservation techniques, enabling cells to be imaged in their near-native state.[43,44]

In a synchrotron facility, SXM imaging can be achieved via a scanning approach (in contrast to full-field imaging) in which x-rays are focused into a small spot (~50-nm diameter or less) that is raster-scanned across the sample. This enables 3D chemical mapping to be performed via x-ray absorption spectroscopy, opening new possibilities for linking chemistry with structure.[45] This is beginning to be exploited for biological materials where, for example, new insights have been obtained for biomineralization[45,46] and the arrangement of proteins in natural fibers.[47,48]

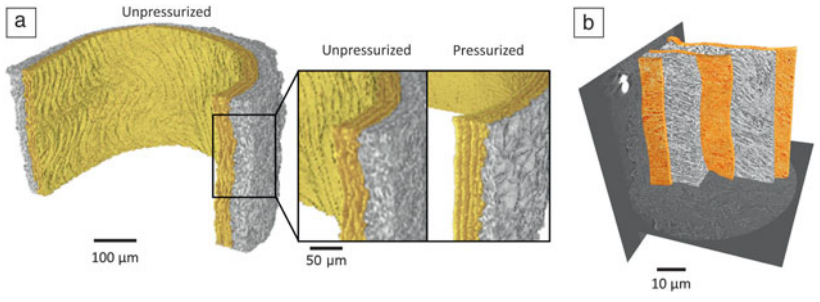


Figure 2. Multiscale x-ray phase-contrast imaging of a rat artery wall. (a) Rendering of the two main layers (media [middle] in yellow, adventitia [outer] in gray) at 1.2-μm resolution, with the concentric lamella in the medial layer shown in yellow. The difference in wall morphology between the unpressurized (0 mm Hg, 0 Pa) and pressurized (110 mm Hg, 14.7 kPa) states is shown in the inset. (b) Higher resolution imaging of three successive lamella (orange) in the media at 150-nm resolution.[17]

https://doi.org/10.1557/mrs.2016.137 Published online by Cambridge University Press

Hierarchical multiscale imaging

Multiscale tomography brings together images from different scales. These can be uncorrelated, where different features are examined and quantified at different scales, or correlated, where a feature is identified at a coarse scale and then studied in greater detail.[7]

Such multiscale approaches can be carried out within the same instrument by using different instruments having the same imaging modality (x-rays), or by combining information from different modalities (see **Figure 3**). Uncorrelated multiscale imaging is much easier to undertake because there is no need to locate and co-register the same volume of interest (which may lie beneath the surface) across different instruments. Uncorrelated imaging is useful when statistical data are required at each scale level (e.g., across the structural scales in bone in Figure 1). If the range of resolutions to be spanned is not too large, correlative multiscale imaging can be carried out using a higher magnification region of interest tomography without cutting up the sample.[49] Walton et al.[17] linked together nano- and micro-CT imaging of an artery wall (Figure 2), without cutting the sample, by performing the nano-CT near the sample surface. In some cases, x-ray imaging can be used to ensure that time-consuming serial sectioning is focused on a region known to contain the feature of interest.

Despite the attractiveness of CT as a part of multiscale imaging schemes, little work has been reported to date, particularly for biological materials, and this is sure to be an area of increased activity going forward. For instance, the possibilities of multiscale imaging of subcellular components by combining soft x-ray microscopy, light microscopy, and 3D SEM techniques are just beginning to be explored.[50]

Multifaceted correlative tomography

Recently, 2D imaging techniques have been combined to provide complementary information on the same surface, or near surface, region of interest. Coined "correlative microscopy,"[51] this approach is now routinely applied in the life sciences, in particular, as a means of combining optical fluorescence microscopy and electron microscopy.[52] Burnett et al.[7] adopted the phrase "correlative tomography" to describe the 3D analogue of this. The approach involves using surface features identified from CT data to locate sub-regions, physically cut from the sample using a focused ion beam, for higher resolution electron imaging or multifaceted analysis. Initially, this was carried out manually, but more recently, semiautomated systems have been developed.[53] Correlative approaches have also been developed to link optical imaging with CT. Handshuh et al.[54] developed a workflow to correlate CT, serial section light microscopy and TEM, using osmium stained tissue.

There is an increasing interest in combining high-resolution imaging modalities in a single instrument, with synchrotron beamlines being particularly suited to this. For instance, fluorescence imaging and soft x-ray tomography have been combined to achieve multimodal imaging of whole cells and subcellular components.[55,56] Liebl et al.[57] combined tomographic imaging of trabecular bone with small-angle x-ray scattering tomography such that morphology and crystal orientation can be related. A natural extension of this is to correlate imaging with microscale mechanical tests such that the local properties of bone can be mapped and related to the collagen orientation.

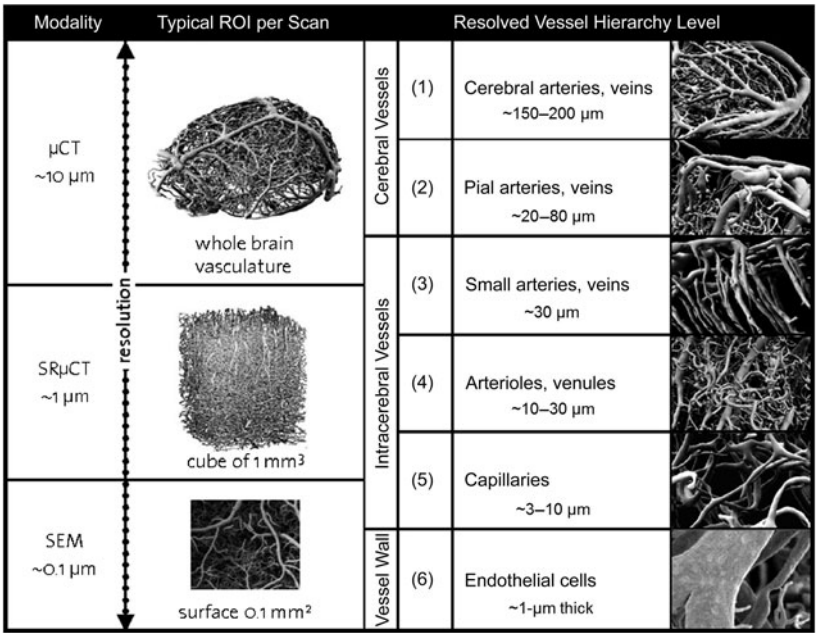


Figure 3. Levels of hierarchy associated with image modalities used for analysis of vascular networks. Each order of magnitude in resolution reveals a new functional level (structure, tissue, and cell). Adapted with permission from Reference 68. © 2006 Elsevier. Note: CT, computed tomography; SR, synchrotron radiation; SEM, scanning electron microscopy; ROI, region of interest.

Temporal (4D) imaging

For many years, the noninvasive nature of CT has been exploited to follow the degradation of man-made materials.[58,59] Attention is starting to focus on natural materials, however, time-lapse x-ray imaging of biological materials is challenging. The mechanical and physical properties are highly dependent on the environment, with dehydration being particularly problematic for soft tissues. Very high doses of x-rays introduce molecular damage that can progressively affect the mechanical properties.[60]

To date, there are relatively few high-resolution 4D studies of biological materials. Lowe et al.[61] used native x-ray absorption contrast to image the development of selected tissues during metamorphosis of a painted lady butterfly over many days. By contrast, Walker et al.[62] used fast synchrotron imaging at much

https://doi.org/10.1557/mrs.2016.137 Published online by Cambridge University Press

shorter extremes to study the dynamics of the flight motor in a living blow fly, which oscillates at 150 Hz (see **Figure 4**).

Studies are starting to emerge exploiting *in situ* loading with CT for biological materials. Jang et al.[63] studied deformation at the micrometer scale in the bone-periodontal ligament during compressive loading, while Wiest et al.[64] combined real-time radiography with tomography to study local deformation under fatigue of a two-piece dental implant. Recently, nanotomography has been used to study progressive crack propagation in beetle cuticle *in situ* under tension (**Figure 5**), giving insights into failure modes and their link to mechanical properties.[65] A notched sample of the beetle elytron (the hardened forewing) was prepared and mounted in a nanomechanical test stage, which enables tomography scans to be taken while the sample is under load. The cuticle has a layered structure in which the orientation of chitin fiber bundles (macrofibers) in successive layers differs by ~90°. Cracks grow through this "cross-ply" structure by displacement of neighboring macrofibers within a layer and by failure of individual macrofibers. The tortuous crack morphology therefore closely follows the orientation of the plies.

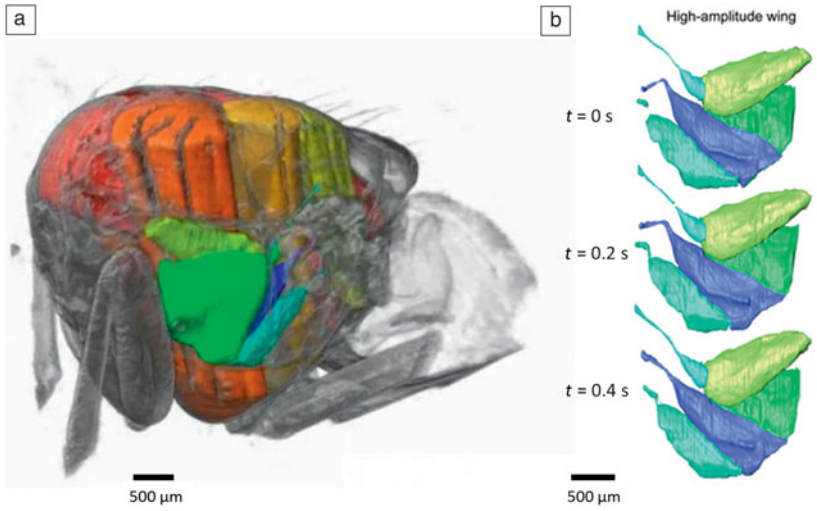


Figure 4. Four-dimensional (4D) imaging of the flight motor in a blow fly. (a) Rendering of the thorax showing power muscles (yellow to red) and steering muscles (green to blue). (b) Rendering of the steering muscles at three time points (*t*) for high-amplitude wing motion. Adapted with permission from Reference 62. © 2014 *PLoS Biology*.

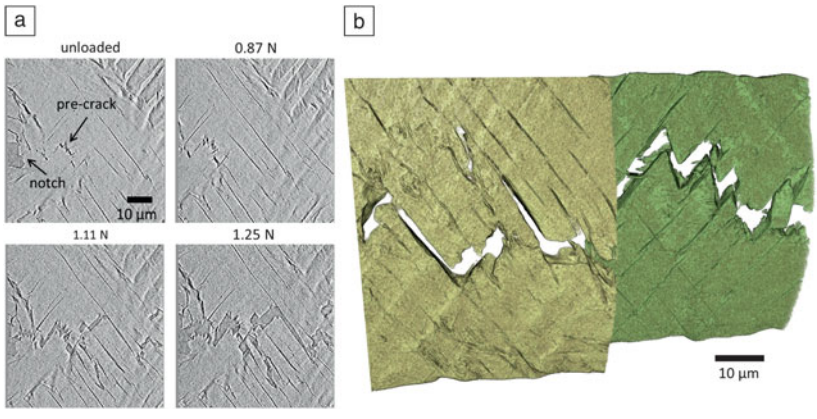


Figure 5. Virtual CT section showing progressive crack growth in beetle cuticle (a) with applied load under tension and (b) with a rendering of the crack path in successive layers shown. The layers overlap, but have been offset horizontally for clarity.[65] The data were obtained by x-ray nanotomography.

Summary and perspectives

In view of the many and varied ways in which the hierarchical structures in biological materials give rise to outstanding and unusual properties, it is surprising that little multiscale 3D or time-lapse (4D) imaging has been carried out to date. Most studies have relied upon a combination of *ex situ* mechanical testing followed by SEM imaging of the fracture surface to try and understand behavior. Recent advances in x-ray imaging technology, coupled with correlative multiscale tomography, promise to change this landscape for studying biological materials and, more broadly, across materials science. Phase-contrast imaging techniques are now available across length scales from hundreds of micrometers to tens of nanometers, but have yet to be linked up within correlative frameworks. There is little doubt that developments in automating the correlation between different instruments and imaging modalities will see a rapid expansion of multiscale, multifaceted correlative imaging approaches in the future, providing a more holistic understanding from macromolecules, through the whole cell architecture and extracellular matrix to the behavior of bulk tissue.

Acknowledgments

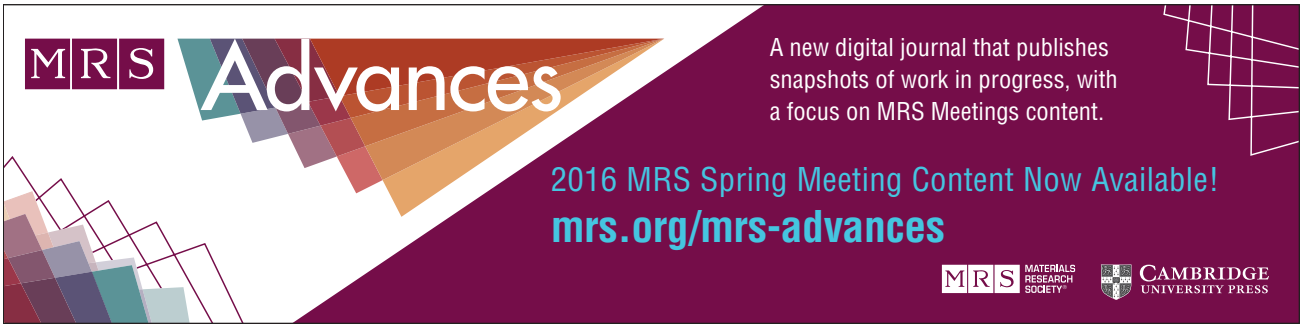
The authors would like to thank EPSRC funding for the Henry Moseley X-Ray Imaging Facility under Grants EP/M010619, EP/K004530, EP/F007906, and EP/F028431. R.S.B. is grateful for Zeiss for funding his research fellowship.

References

1. P. Fratzl, R. Weinkamer, *Prog. Mater. Sci.* **52**, 1263 (2007).
2. A.H. Barber, D. Lu, N.M. Pugno, *J. R. Soc. Interface* **12**, 20141326 (2015).
3. M.A. Meyers, P.-Y. Chen, M.I. Lopez, Y. Seki, A.Y.M. Lin, *J. Mech. Behav. Biomed. Mater.* **4**, 626 (2011).
4. J.F.V. Vincent, *Proc. Inst. Mech. Eng. H J. Eng. Med.* **223**, 919 (2009).
5. Q. Chen, N.M. Pugno, *J. Mech. Behav. Biomed. Mater.* **19**, 3 (2013).
6. F. Barthelat, *Int. Mater. Rev.* **60**, 413 (2015).
7. T.L. Burnett, S.A. McDonald, A. Gholinia, R. Geurts, M. Janus, T. Slater, S.J. Haigh, C. Ornek, F. Almuaili, D.L. Engelberg, G.E. Thompson, P.J. Withers, *Sci. Rep.* **4**, 4711 (2014).
8. V. Ntziachristos, *Nat. Methods* **7**, 603 (2010).
9. J.J. Socha, M.W. Westneat, J.F. Harrison, J.S. Waters, W.-K. Lee, *BMC Biol.* **5**, 1 (2007).

https://doi.org/10.1557/mrs.2016.137 Published online by Cambridge University Press

10. M.R. Howells, T. Beetz, H.N. Chapman, C. Cui, J.M. Holton, C.J. Jacobsen, J. Kirz, E. Lima, S. Marchesini, H. Miao, D. Sayre, D.A. Shapiro, J.C.H. Spence, D. Starodub, *J. Electron. Spectrosc. Relat. Phenom.* **170**, 4 (2009).
11. R. Carzaniga, M.-C. Domart, L.M. Collinson, E. Duke, *Protoplasma* **251**, 449 (2014).
12. B. Alberto, C. Paola, S. Pekka, *Phys. Med. Biol.* **58**, R1 (2013).
13. S. Zabler, P. Cloetens, J.-P. Guigay, J. Baruchel, M. Schlenker, *Rev. Sci. Instrum.* **76**, 073705 (2005).
14. T. Weitkamp, A. Diaz, C. David, F. Pfeiffer, M. Stampanoni, P. Cloetens, E. Ziegler, *Opt. Express* **13**, 6296 (2005).
15. A. Tkachuk, F. Duewer, H. Cui, M. Feser, S. Wang, W. Yun, *Z. Kristallogr. Cryst. Mater.* **222**, 650 (2007).
16. C.K. Hagen, P. Maghsoudlou, G. Totonelli, P.C. Diemoz, M. Endrizzi, L. Rigon, R.-H. Menk, F. Arfelli, D. Dreossi, E. Brun, P. Coan, A. Bravin, P. De Coppi, A. Olivo, *Sci. Rep.* **5**, 18156 (2015).
17. L.A. Walton, R.S. Bradley, P.J. Withers, V.L. Newton, R.E.B. Watson, C. Austin, M.J. Sherratt, *Sci. Rep.* **5**, 10074 (2015).
18. G. Poologasundarampillai, D. Wang, S. Li, J. Nakamura, R. Bradley, P.D. Lee, M.M. Stevens, D.S. McPhail, T. Kasuga, J.R. Jones, *Acta Biomater.* **10**, 3733 (2014).
19. F. Pfeiffer, T. Weitkamp, O. Bunk, C. David, *Nat. Phys.* **2**, 258 (2006).
20. G. Schulz, T. Weitkamp, I. Zanette, F. Pfeiffer, F. Beckmann, C. David, S. Rutishauser, E. Reznikova, B. Müller, *J. R. Soc. Interface* **7**, 1665 (2010).
21. I. Zanette, T. Zhou, A. Burvall, U. Lundström, D.H. Larsson, M. Zdora, P. Thibault, F. Pfeiffer, H.M. Hertz, *Phys. Rev. Lett.* **112**, 253903 (2014).
22. H. Wang, Y. Kashyap, K. Sawhney, *Sci. Rep.* **6**, 20476 (2016).
23. M. Langer, A. Pacureanu, H. Suhonen, Q. Grimal, P. Cloetens, F. Peyrin, *PLoS One* **7**, e35691 (2012).
24. S. Marchesini, H.N. Chapman, S.P. Hau-Riege, R.A. London, A. Szoke, H. He, M.R. Howells, H. Padmore, R. Rosen, J.C.H. Spence, U. Weierstall, *Opt. Express* **11**, 2344 (2003).
25. F. Berenguer, R.J. Bean, L. Bozec, J. Vila-Comamala, F. Zhang, C.M. Kewish, O. Bunk, J.M. Rodenburg, I.K. Robinson, *Biophys. J.* **106**, 459 (2014).
26. I. Zanette, B. Enders, M. Dierolf, P. Thibault, R. Gradl, A. Diaz, M. Guizar-Sicairos, A. Menzel, F. Pfeiffer, P. Zaslansky, *Sci. Rep.* **5**, 9210 (2015).
27. M. Dierolf, A. Menzel, P. Thibault, P. Schneider, C.M. Kewish, R. Wepf, O. Bunk, F. Pfeiffer, *Nature* **467**, 436 (2010).
28. K. Giewekemeyer, C. Hackenberg, A. Aquila, R.N. Wilke, M.R. Groves, R. Jordanova, V.S. Lamzin, G. Borchers, K. Saksl, A.V. Zozulya, M. Sprung, A.P. Mancuso, *Biophys. J.* **109**, 1986 (2015).
29. L. Shemilt, E. Verbanis, J. Schwenke, A.K. Estandarte, G. Xiong, R. Harder, N. Parmar, M. Yusuf, F. Zhang, I.K. Robinson, *Biophys. J.* **108**, 706 (2015).
30. B.D. Metscher, *BMC Physiol.* **9**, 1 (2009).
31. P. Das Neves Borges, A.E. Forte, T.L. Vincent, D. Dini, M. Marenzana, *Osteoarthr. Cartil.* **22**, 1419 (2014).
32. T.D. Butters, S.J. Castro, T. Lowe, Y. Zhang, M. Lei, P.J. Withers, H. Zhang, *PLoS One* **9**, e105552 (2014).
33. O.V. Aslanidi, T. Nikolaidou, Z. Jichao, B.H. Smaill, S.H. Gilbert, A.V. Holden, T. Lowe, P.J. Withers, R.S. Stephenson, J.C. Jarvis, J.C. Hancox, M.R. Boyett, Z. Henggui, *IEEE Trans. Med. Imaging* **32**, 8 (2013).
34. T. Shearer, S. Rawson, S.J. Castro, R. Balint, R.S. Bradley, T. Lowe, J. Vila-Comamala, P.D. Lee, S.H. Cartmell, *Muscles Ligaments Tendons J.* **4**, 238 (2014).
35. J.M. de Silva, I. Zanette, P.B. Noël, M.B. Cardoso, M.A. Kimm, F. Pfeiffer, *Sci. Rep.* **5**, 14088 (2015).
36. L.E. Cole, R.D. Ross, J.M.R. Tilley, T. Vargo-Gogola, R.K. Roeder, *Nanomedicine* **10**, 321 (2015).
37. J.C. De La Vega, U.O. Häfeli, *Contrast Media Mol. Imaging* **10**, 81 (2015).
38. R. Popovtzer, A. Agrawal, N.A. Kotov, A. Popovtzer, J. Balter, T.E. Carey, R. Kopelman, *Nano Lett.* **8**, 4593 (2008).
39. C. Hagen, S. Werner, S. Carregal-Romero, A.N. Malhas, B.G. Klupp, P. Guttmann, S. Rehbein, K. Henzler, T.C. Mettenleiter, D.J. Vaux, W.J. Parak, G. Schneider, K. Grunewald, *Ultramicroscopy* **146**, 46 (2014).
40. P.J. Withers, *Mater. Today* **10**, 26 (2007).
41. M. Bertilson, O. von Hofsten, U. Vogt, A. Holmberg, A.E. Christakou, H.M. Hertz, *Opt. Lett.* **36**, 2728 (2011).
42. D.B. Carlson, J. Gelb, V. Palshin, J.E. Evans, *Microsc. Microanal.* **19**, 22 (2013).
43. M. Uchida, Y. Sun, G. McDermott, C. Knoechel, M.A. Le Gros, D. Parkinson, D.G. Drubin, C.A. Larabell, *Yeast* **28**, 227 (2011).
44. G. Schneider, P. Guttmann, S. Heim, S. Rehbein, F. Mueller, K. Nagashima, J.B. Heymann, W.G. Muller, J.G. McNally, *Nat. Methods* **7**, 985 (2010).
45. M. Obst, G. Schmid, "3D Chemical Mapping: Application of Scanning Transmission (Soft) X-Ray Microscopy (STXM) in Combination with Angle-Scan Tomography in Bio-, Geo-, and Environmental Sciences," in *Electron Microscopy: Methods and Protocols*, J. Kuo, Ed. (Humana Press, Totowa, NJ, 2014) pp. 757–781.
46. J. Cosmidis, K. Benzerara, N. Nassif, T. Tyliszczak, F. Bourdelle, *Acta Biomater.* **12**, 260 (2015).
47. D. Hernández Cruz, M.-E. Rousseau, M.M. West, M. Pézolet, A.P. Hitchcock, *Biomacromolecules* **7**, 836 (2006).
48. J. Normandeau, C. Van Kessel, D. Nicholson, B. Rahusaar Routledge, A. Fawcett, L. Lim-Cole, C. Condy, N. Sylvain, T. Walker, F. Borondics, *Can. Young Sci. J.* **2014**, 35 (2014).
49. A. Kyrieleis, V. Titarenko, M. Ibison, T. Connolley, P.J. Withers, *J. Microsc.* **241**, 69 (2011).
50. A. Patwardhan, A. Ashton, R. Brandt, S. Butcher, R. Carzaniga, W. Chiu, L. Collinson, P. Doux, E. Duke, M.H. Ellisman, E. Franken, K. Grunewald, J.-K. Heriche, A. Koster, W. Kuhlbrandt, I. Lagerstedt, C. Larabell, C.L. Lawson, H.R. Saibil, E. Sanz-Garcia, S. Subramaniam, P. Verkade, J.R. Swedlow, G.J. Kleywegt, *Nat. Struct. Mol. Biol.* **21**, 841 (2014).
51. J. Caplan, M. Niethammer, R.M. Taylor, K.J. Czymmek, *Curr. Opin. Struct. Biol.* **21**, 686 (2011).
52. B.N.G. Giepmans, *Histochem. Cell Biol.* **130**, 211 (2008).
53. A. Merkle, L. Lechner, A. Steinbach, J. Gelb, M. Kienle, M. Phaneuf, D. Unrau, S. Singh, N. Chawla, *Microsc. Anal.* **28**, S10 (2014).
54. S. Handschuh, N. Baeumler, T. Schwaha, B. Ruthensteiner, *Front. Zool.* **10**, 1 (2013).
55. G. Schneider, P. Guttmann, S. Rehbein, S. Werner, R. Follath, *J. Struct. Biol.* **177**, 212 (2012).
56. E.A. Smith, G. McDermott, M. Do, K. Leung, B. Panning, M. Le Gros, C.A. Larabell, *Biophys. J.* **107**, 1988 (2014).
57. M. Liebi, M. Georgiadis, A. Menzel, P. Schneider, J. Kohlbrecher, O. Bunk, M. Guizar-Sicairos, *Nature* **527**, 349 (2015).
58. P.J. Withers, M. Preuss, *Annu. Rev. Mater. Res.* **42**, 81 (2012).
59. E. Maire, P.J. Withers, *Int. Mater. Rev.* **59**, 1 (2014).
60. H.D. Barth, E.A. Zimmermann, E. Schaible, S.Y. Tang, T. Alliston, R.O. Ritchie, *Biomaterials* **32**, 8892 (2011).
61. T. Lowe, R.J. Garwood, T.J. Simonsen, R.S. Bradley, P.J. Withers, *J. R. Soc. Interface* **10**, 20130304 (2013).
62. S.M. Walker, D.A. Schwyn, R. Mokso, M. Wicklein, T. Müller, M. Doube, M. Stampanoni, H.G. Krapp, G.K. Taylor, *PLoS Biol.* **12**, e1001823 (2014).
63. A.T. Jang, J.D. Lin, Y. Seo, S. Etchin, A. Merkle, K. Fahey, S.P. Ho, *J. Vis. Exp.* **85**, e51147 (2014).
64. W. Wiest, S. Zabler, A. Rack, C. Fella, A. Balles, K. Nelson, R. Schmelzeisen, R. Hanke, *J. Synchrotron Radiat.* **22**, 1492 (2015).
65. B. Patterson, N.L. Cordes, K. Henderson, J.C.E. Mertens, A.J. Clarke, X. Lu, R. Hartwell, B. Hornberger, A. Merkle, S. Etchin, A. Tkachuk, M. Leibowitz, D. Trapp, W. Qiu, B. Zhang, H. Bale, P.J. Withers, R.S. Bradley, *Exp. Mech.* (forthcoming).
66. U.G.K. Wegst, H. Bai, E. Saiz, A.P. Tomsia, R.O. Ritchie, *Nat. Mater.* **14**, 23 (2015).
67. A. Ilnicka, J.P. Lukaszewicz, *Front. Mater.* **2**, 20 (2015), doi:10.3389/fmats.2015.00020.
68. S. Heinzer, T. Krucker, M. Stampanoni, R. Abela, E.P. Meyer, A. Schuler, P. Schneider, R. Müller, *Neuroimage* **32**, 626 (2006). □



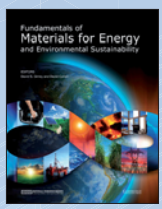
https://doi.org/10.1557/mrs.2016.137 Published online by Cambridge University Press

Recent Titles

from the Materials Research Society
and Cambridge University Press

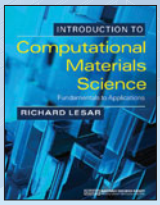
Book Collection

TEXTBOOKS



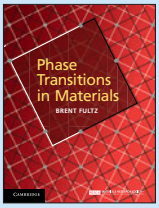
Fundamentals of Materials for Energy and Environmental Sustainability

EDITORS: David S. Ginley and David Cahen
ISBN: 9781107000230
List Price: $110.00
MRS Member Price: $88.00
www.cambridge.org/ginley



Introduction to Computational Materials Science
Fundamentals to Applications

AUTHOR: Richard LeSar
ISBN: 9780521845878
List Price: $100.00
MRS Member Price: $80.00
www.cambridge.org/lesar



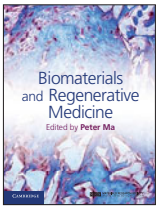
Phase Transitions in Materials

AUTHOR: Brent Fultz
ISBN: 9781107067240
List Price: $105.00
MRS Member Price: $84.00
www.cambridge.org/fultz



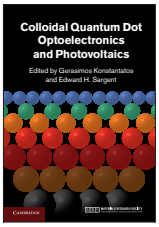
Biological Materials Science
Biological Materials, Bioinspired Materials, and Biomaterials

AUTHORS: Marc André Meyers and Po-Yu Chen
ISBN: 9781107010451
List Price: $110.00
MRS Member Price: $88.00
www.cambridge.org/bms



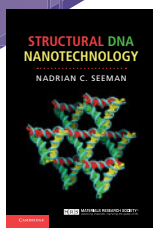
Biomaterials and Regenerative Medicine

EDITOR: Peter Ma
ISBN: 9781107012097
List Price: $195.00
MRS Member Price: $156.00
www.cambridge.org/biomaterials



Colloidal Quantum Dot Optoelectronics and Photovoltaics

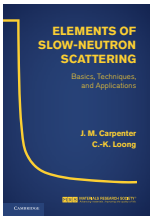
EDITORS: Gerasimos Konstantatos and Edward H. Sargent
ISBN: 9780521198264
List Price: $140.00
MRS Member Price: $112.00
www.cambridge.org/colloidal



NEW
2016 PROSE Award Winner in Biological Science

Structural DNA Nanotechnology

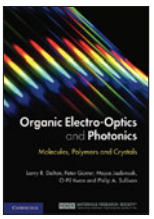
AUTHOR: Nadrian C. Seeman
ISBN: 9780521764483
List Price: $65.00
MRS Member Price: $52.00
www.cambridge.org/seeman



NEW

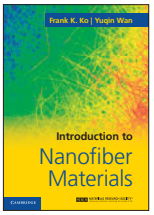
Elements of Slow-Neutron Scattering
Basics, Techniques, and Applications

AUTHORS: J. M. Carpenter and C.-K. Loong
ISBN: 9780521857819
List Price: $175.00
MRS Member Price: $140.00
www.cambridge.org/carpenter



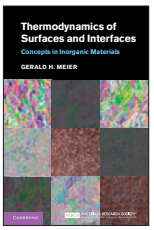
Organic Electro-Optics and Photonics
Molecules, Polymers, and Crystals

AUTHORS: Larry R. Dalton, Peter Günter, Mojca Jazbinsek, O-Pil Kwon and Philip A. Sullivan
ISBN: 9780521449656
List Price: $80.00
MRS Member Price: $64.00
www.cambridge.org/dalton



Introduction to Nanofiber Materials

AUTHORS: Frank K. Ko and Yuqin Wan
ISBN: 9780521879835
List Price: $115.00
MRS Member Price: $92.00
www.cambridge.org/nanofiber



Thermodynamics of Surfaces and Interfaces
Concepts in Inorganic Materials

AUTHOR: Gerald H. Meier
ISBN: 9780521879088
List Price: $140.00
MRS Member Price: $112.00
www.cambridge.org/meier

To view the entire collection, visit
www.cambridge.org/mrs-cambridge

Enter Discount Code **MRSMEMBER** at checkout to apply the MRS Member discount for these and all Cambridge science/engineering books and proceedings.

Not an MRS Member? Join today at **www.mrs.org/join.**

MRS MATERIALS RESEARCH SOCIETY®

CAMBRIDGE UNIVERSITY PRESS

https://doi.org/10.1557/mrs.2016.137 Published online by Cambridge University Press

MRS ENERGY & SUSTAINABILITY

A Review Journal

TOPICS CONTROVERSIAL EXPERT REVIEWS



MRS Energy & Sustainability—A Review Journal publishes reviews on key topics in materials research and development as they relate to energy and sustainability. Review topics include new R&D of both established and new areas; systems integration; and objective application of economic, sociological and governmental models, enabling research and technological developments. The reviews are set in an integrated context of scientific, technological and sociological complexities relating to environment and sustainability.

EDITORS-IN-CHIEF

David S. Ginley
National Renewable Energy Laboratory, USA

David Cahen
Weizmann Institute of Science, Israel

Elizabeth A. Kócs
University of Illinois at Chicago, USA

www.mrs.org/energy-sustainability-journal

https://doi.org/10.1557/mrs.2016.137 Published online by Cambridge University Press